Wear characteristics of spray formed Al-alloys and their composites

V. C. Srivastava · G. B. Rudrakshi ·
V. Uhlenwinkel · S. N. Ojha

Abstract In the present investigation, different Al based alloys such as Al–Si–Pb, Al–Si, Al–Si–Fe and 2014Al + SiC composites have been produced by spray forming process. The microstructural features of monolithic alloys and composite materials have been examined and their wear characteristics have been evaluated at different loads and sliding velocities. The microstructural features invariably showed a significant refinement of the primary phases and also modification of secondary phases in Al-alloys. The Pb particles in Al–Si–Pb alloy were observed to be uniformly distributed in the matrix phase besides decorating the grain boundaries. The spray formed composites showed uniform distribution of SiC particles in the matrix. It was observed that wear resistance of Al–Si alloy increases with increase in Pb content; however, there is not much improvement after addition of Pb more than 20%. The coefficient of friction reduced to 0.2 for the alloy containing 20%Pb. A sliding velocity of 1 ms^{-1} was observed to be optimum for high wear resistance of these materials. Alloying elements such as Fe and Cu in Al–Si alloy lead to improved wear resistance compared to that of the base alloy. The addition of SiC in 2014Al alloy gave rise to considerable improvement in wear resistance but primarily in the low pressure regime. The wear rate seemed to decrease with increase in sliding velocity. The wear response of the materials has been discussed in light of their microstructural features and topographical observation of worn surfaces.

Introduction

In the past few years, the material specifications for applications requiring high wear resistance have become more stringent due to increased recurring costs and the requirement of unprecedented performance. Although there have been a number of investigations focused on the development of such materials, the major emphasis has been given to composite materials in the last few years. In one of the approaches, relatively hard matrix is embedded with fine distribution of a soft phase, and in the other, hard second phase particles are introduced in a soft matrix [1–3]. And also, recently, the demand for light weight wear resistant materials for automotive and aerospace application has seen a paradigm shift. To cater to such necessity, Al alloys based composites with either soft or hard reinforcing particles have been envisaged as the potential candidate materials [4–9]. The potential material systems to satisfy above criteria are liquid immiscible Al–Pb system (Pb as a soft phase), hypereutectic Al–Si alloys and Al–SiC metal matrix composites.

However, liquid immiscible alloys having component phases with large density difference are difficult to produce by conventional processes [6]. This is due to the fact that

V. C. Srivastava
Metal Extraction & Forming Division, National Metallurgical Laboratory, Jamshedpur 831007, India

V. C. Srivastava · V. Uhlenwinkel
Institut für Werkstofftechnik, Universität Bremen, 28359 Bremen, Germany

G. B. Rudrakshi
Department of Mechanical Engineering, Basaveshwar Engineering College, Bagalkot 587102, India

S. N. Ojha (✉)
Department of Metallurgical Engineering, Banaras Hindu University, Varanasi 221005, India
e-mail: snojha@rediffmail.com

slow cooling rate during conventional casting processes leads to phase separation in liquid state and segregation of minor phase due to high density. The slow cooling rate also gives considerable time for coalescence of precipitating liquid phase. Therefore, efficient processing of such materials by conventional route is truly difficult. Similarly, conventional casting processes for achieving refined size and uniform distribution of primary Si phase and modified eutectic Si in hypereutectic Al–Si alloys has been proved to be non-sufficient, particularly for alloys with higher Si content [10, 11]. On the other hand, incorporation of fine second phase ceramic particles in liquid poses limitations due to poor wetting ability of most ceramics with liquid metal. Poor wettability of ceramic particles leads to clustering of small size particles in the melt. In addition, the high temperature involved in conventional casting processes leads to deleterious reaction products at the reinforcement/matrix interfaces that deteriorate the properties [5, 12].

The spray forming process has been observed to obviate most of the above limitations associated with processing of liquid immiscible alloys [4], non-conventional Al–Si alloys [13–16] and metal matrix composites [17–19] by conventional routes. This process employs disintegration of liquid metal into a spray of micron size droplets using high velocity inert gas jet. The spray is then collected over a substrate to give rise to a dense perform [20, 21]. The small size droplets in the spray experience a high cooling rate due to increased surface to volume ratio and the forced convection in the high velocity gas jet. The incoming spray on a growing preform gives rise to a semi-solid/liquid pool on the top surface restricting the scale of segregation of precipitating phases. The combination of high cooling rate and unique microstructural evolution process makes the spray forming process suitable for designing new materials.

The new schemes, given by the authors, of incorporation of Pb in liquid melt to avoid high temperature of single phase liquid region [4] and of ceramic particles in the spray cone [22] during spray forming have given rise to comparatively better microstructural features, which are expected to give better wear characteristics compared to conventionally processed alloys. Although, a number of studies have been carried out on the wear behaviour of Al alloys and their composites, these are mostly on the conventionally processed materials. Only a few studies are available that report wear behaviour of spray formed alloy and composites such as Al–Si alloy [23–26], Al based liquid immiscible alloys [4, 27] and Al matrix composites [28, 29]. In addition, the variation in processing and test condition makes it difficult to compare their wear resistance. Therefore, in view of this, attempt has been made to produce Al–Si, Al–Si–Pb and 2014-Al + SiC composites materials using spray forming process, with a view to have a comparative study of wear behaviour of these materials. The alloy systems and composites have been chosen for this study due to their highly relevant wear properties for automotive applications. A comparison of their wear behaviour will add to the understanding of the effect of their microstructural features on wear characteristics.

Experimental details

Spray forming

The spray forming of Al–6.5Si, Al–18Si, Al–18Si–5Fe–1.5Cu and Al–Cu–Si–Pb alloys was carried out using a convergent–divergent close-coupled nozzle assembly. The schematic representation of the spray forming setup used is shown in the Ref. [4]. In brief, the alloy was melted in a graphite crucible using a resistance heating furnace. The spray was deposited over a copper substrate, centered along the spray axis, to achieve disc shape perform of 170 mm diameter with a height of 70 mm. The process parameters used in the synthesis of the materials are given in Table 1.

The spray forming setup used for the metal matrix composites is shown and discussed elsewhere [22]. The spray forming of composites was carried out at the University of Bremen (Germany) in the spray forming plant SK-2. The setup consisted of a tundish, a freefall scanning nozzle assembly, a particle dispenser, a substrate and an atomization chamber. The SiC particulate reinforcement was incorporated in the atomization zone by a powder

Table 1 Process parameters used for spray forming of various alloys

Alloy composition	Gas pressure, MPa	Gas/melt flow ratio	Melt temperature, °C	Deposition distance, m
Al–3.5Cu–10Si	1.0	0.89	750	0.45
Al–3.5Cu–10Si–20Pb	1.0	0.85	750	0.45
Al–3.5Cu–10Si–10Pb	1.0	0.85	750	0.45
Al–3.5Cu–10Si–30Pb	1.0	0.83	750	0.45
Al–6.5Si	1.2	1.24	800	0.30
Al–18Si	1.2	1.24	950	0.30
Al–18Si–5Fe–1.5Cu	1.2	1.16	975	0.30

feeding system through a particle dispenser. The powder feeding system consisted of a hopper and a screw conveyor enclosed in a pressurized chamber. The powder was conveyed to the particle dispenser with high velocity nitrogen gas and fed into the atomization zone using a concentric annular channel in the atomization nozzle. The nominal composition of the alloy used as matrix was Al–4.5Cu–1.0Si–0.5 Mg (wt.%). The required amount of each element (total 45 kg) was melted together in a crucible in an induction furnace under a nitrogen cover and poured into the tundish. The melting temperature was 735 °C. A gas to melt flow rate ratio of 2.47 (melt flow rate: 330 kg/h) was used in all the experiments. The liquid melt is atomized by nitrogen gas and simultaneously reinforcement powder particles are fed into the atomization zone. Composites were produced using different particle sizes (6–58 μm) and volume fraction (5–12%). The detailed characteristics of the billet material can be seen in our other publications [30].

Wear testing

The wear testing of spray formed alloys and composite was carried out on a DUCOM (Bangalore, India) make pin-on-disc type wear testing machine. The setup employed a hardened steel disk with hardness value of 52Rc and a specimen holder. Wear testing was done on cylindrical specimen pin with 8 mm diameter and 30 mm length. The details of the wear test setup are given elsewhere [4]. The wear length of the sample was measured through a linear variable differential transducer (LVDT). The wear volume was calculated considering the diameter of the specimen and wear length. The frictional force on the specimen was measured using a load cell attached to the setup. This measures the force component of the moment acting on the specimen. The standard wear test procedure was followed for evaluating the wear rate at different loads and sliding speeds. The disc surface was cleaned with acetone before each experimental run. All tests were carried out in dry sliding conditions and at room temperature. The worn out surfaces were kept for further examination. The temperature of the wear surface of the specimen was measured 2 mm above the surface using a thermocouple.

Results

Microstructure

Al–10Si–3.5Cu alloy with Pb

The microstructure of Al–3.5Cu–10Si alloy invariably exhibited equiaxed grain morphology of the primary α-phase with particulate morphology of Si particles located at the grain boundaries and finer Si particles in the grain interior (Fig. 1a). A variation in grain size of primary α-phase and Si particles on the grain boundaries in different sections of the deposit was observed, particularly in the bottom of the deposit and peripheral regions. However, as the steady state deposition condition is achieved, the grain size of α-Al varies in the range of 12–18 μm with a variation in size of Si particles from

Fig. 1 Micrographs of spray formed Al–3.5Cu–10Si alloy produced at a deposition distance of 0.45 m (**a**) without Pb, (**b**) 10% Pb, (**c**) 20%Pb and (**d**) 30%Pb
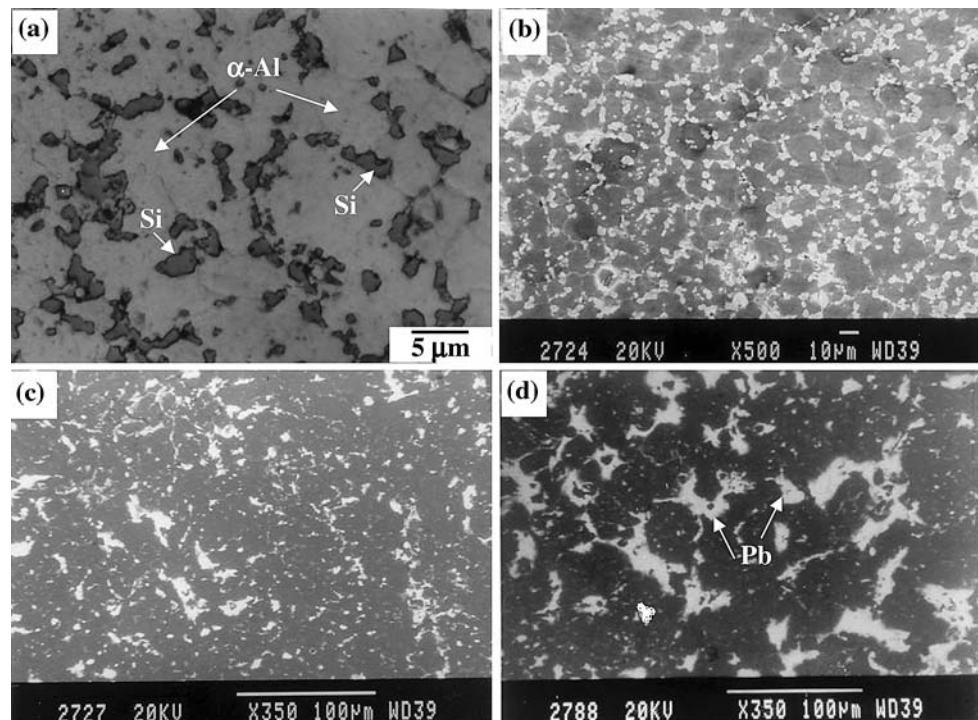
1 to 7 μm. Figure 1b shows the microstructural features of the spray deposited Al–3.5Cu–10Si–10Pb alloy that depicts typical equiaxed grain morphology of the primary α-Al phase. The average grain size is around 20 μm. The grain boundaries are decorated with round Pb particles along with eutectic Si. Figure 1c shows the morphology and distribution of lead particles of Al–3.5Cu–10Si–20Pb alloy in the spray-deposit. There is a large variation in size of the lead particles from 0.5 to 10 μm. The micrograph clearly depicts that some of small lead particles are present within the Al grains. The coalescence of smaller Pb particles may take place during solidification as a consequence of long freezing time and larger volume fraction of Pb. On the other hand, spheroidization of lead particle is hindered due to the fact that the Pb solidifies quite later because of its low freezing temperature. Figure 1d shows the morphology of lead phase in the spray deposited Al–3.5Cu–10Si–30Pb alloy. The large size lead particles are situated at the grain junctions with their tails along the grain boundary. Some of the lead particles are interconnected around Al grains. This region of the spray-deposit showed fine globular eutectic Si particles varying from 1 to 3 μm. The distribution of these Si particles is mostly confined to grain boundaries. However, the triple points are occupied by the lead phase. This feature is in contrast to that observed in the spray deposits of alloy containing 10% Pb.

Al–Si alloys

Figure 2 shows the microstructures of as-spray formed Al–Si alloys. Figure 2a shows fine equiaxed α-Al grains with eutectic Si at the grain boundaries, in Al–6.5Si alloy. The micrograph reveals that eutectic Si possesses a needle-like morphology at the grain boundaries. The grain size varies in the range of 20–30 μm. In contrast, the Al–18Si alloy shows refined primary Si phase in the size range of 5–8 μm (Fig. 2b). It is difficult to distinguish between primary and eutectic Si phases in the spray-deposit of this alloy. This feature is in contrast to the large size cuboids of primary Si phase generally observed in conventionally cast hypereutectic Al–Si alloys [31]. Figure 2c shows the microstructure of spray formed Al–18Si–5Fe–1.5Cu alloy. This reveals refined structure and uniform distribution of primary Si phase and intermetallic compounds such as β-Al_5FeSi and δ-Al_4Si_2Fe phases. The detail investigations led to the conclusion of the presence of intermetallic compounds in Al–18Si–5Fe–1.5Cu alloy, is given in Ref. [32]. The Si phase exhibits gray contrast compared to bright contrast of intermetallic compounds. A significant reduction in the intermetallic phases is the major advantage derived from spray forming of this alloy. In general, these compounds show long plate-like morphology in conventionally cast alloy.

2014-Al + SiC composites

The microstructures of spray formed particulate reinforced 2014-Al + SiC composites in un-etched condition are shown in Fig. 3a–d. The microstructures of composite consist of both smaller as well as larger second phase particles uniformly distributed in the matrix. However, in

Fig. 2 Micrographs of as-spray formed (**a**) Al–6.5Si, (**b**) Al–18Si and (**c**) Al–18Si–5Fe–1.5Cu alloy. Al–Fe–Si intermetallics are in white contrast in **c**
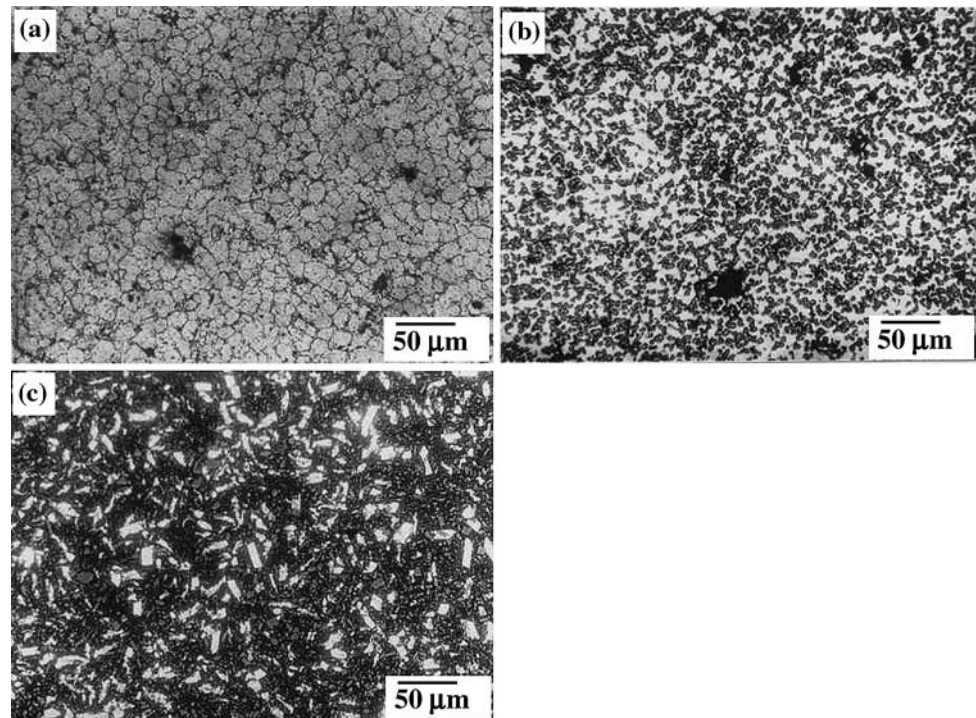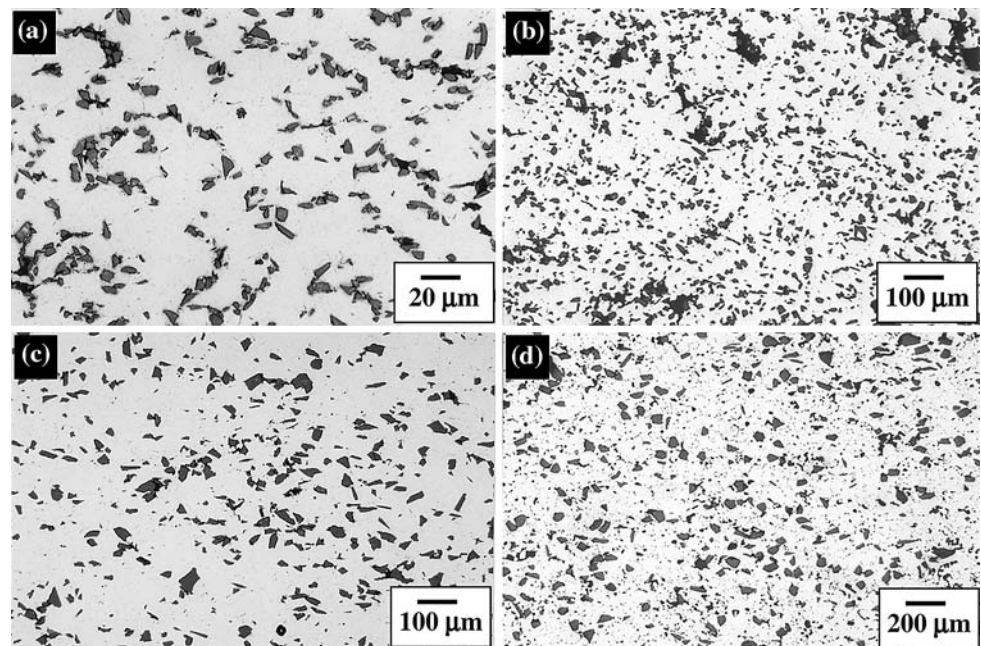
Fig. 3 Typical optical micrographs of 2014-Al + SiC composites with reinforcement size of (**a**) 6 μm, (**b**) 17 μm, (**c**) 30 μm and (**d**) 58 μm

the case of small size reinforcements, particles are found to decorate the grain boundaries and sometimes form small clusters. Whereas, large size particles do not show the tendency of segregation at grain boundaries. The grain size of composites is strongly affected by the size and volume fraction of particles in the matrix. The grain size decreases with increase in volume fraction. However, this feature is often observed to be more sensitive to smaller size range of reinforcements compared to that of large size particles. An increase in volume fraction of 30 μm size particles up to 11% is shown to decrease the grain size from 45 μm in un-reinforced alloy to 30 μm in the composite. Whereas, a 8.4 vol.% of 6 μm size particle gives rise to an average grain size of 17 μm. The porosity level in the composites is observed to be in the range of 5–6 vol.%. However, after hot rolling to 50% thickness reduction, the porosity level is decreased to 1.0–3.0 vol.%. The samples for wear testing were taken from the hot rolled composite plates after solution treatment at 502 °C for 1 h and ageing at 170 °C for 2 h (Fig. 3).

Wear behaviour

Al–10Si–3.5Cu alloy with Pb

Figure 4a shows the variation in wear rate of the alloys with applied pressure. It is obvious from the figure that the wear rate of Al–10Si–3.5Cu alloy increases with increase in applied pressure. The wear rate varies from 1.25 to 6.42×10^{-12} m^3 m^{-1} for a range of applied pressure of 0.2–1.8 MPa. The wear rate typically shows an almost linear variation with applied pressure. The wear rates of

lead dispersed alloys consistently showed lower wear rate compared to that of Al–10Si–3.5Cu alloy. Although the wear rates are comparable in the lower range of applied pressure, there is a marked improvement in higher pressure regime, particularly for an increase of Pb content from 10 to 20%.

Figure 4b shows the variation in coefficient of friction (μ) with applied pressure. The coefficient of friction is observed to decrease initially in the low pressure regime. Subsequently, there is a drastic change in the rate of decrease of coefficient of friction. The value of μ for all the lead compositions finally falls in the range of 0.17–0.40 at an applied pressure of 1.8 MPa, which varied between 0.55 and 0.75 at low pressure of 0.2 MPa. This higher coefficient of friction for lower applied pressure of 0.2 MPa may be due to asperity locking where true contact of the full surface is not established. It is obvious from this figure that the average coefficient of friction is highest for Al–10Si–3.5Cu base alloy with no lead dispersion. The Al–10Si–3.5Cu–10Pb alloy shows small decrease in coefficient of friction whereas the alloy with 20% Pb dispersion shows large decrease in coefficient of friction. However, the decrease in μ for 30% Pb alloy again reduced. Hence, it can be concluded that an optimum composition of lead gives maximum reduction in coefficient of friction which in turn leads to minimum wear.

Figure 5a shows the variation of wear rate with sliding speed for Al–10Si–3.5Cu spray deposited alloys with and without lead dispersion at a constant pressure of 1.0 MPa. The wear rate decreases with increasing sliding velocity, reaches a minimum value at a critical sliding velocity and then increases with further increase in the sliding speed. It
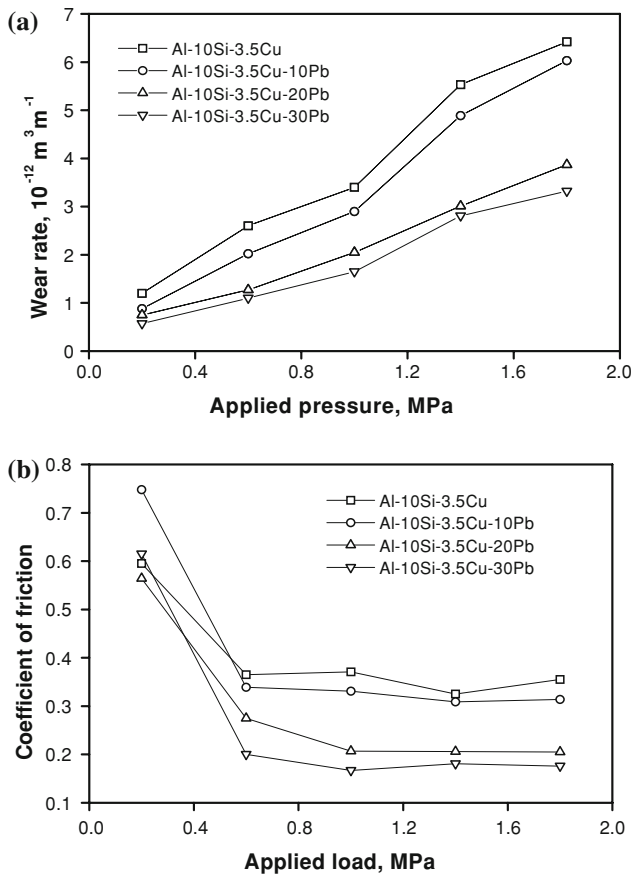
Fig. 4 Variation of (**a**) wear rate and (**b**) coefficient of friction with applied load for spray formed alloys containing varying amount of Pb (constant sliding velocity of 1.0 ms^{-1})

Fig. 5 Variation of (**a**) wear rate and (**b**) coefficient of friction with sliding velocity for spray formed alloys containing varying amount of Pb (constant applied pressure of 1.0 MPa)

is obvious from the above figure that the nature of variation in wear rate for both the base alloys and the alloys with lead dispersion is similar, irrespective of their compositions. However, the alloys with lead dispersion exhibited lower wear rate, which further decreased with increasing Pb content.

Figure 5b shows the variation in coefficient of friction with sliding velocity at an applied pressure of 1.0 MPa. The coefficient of friction (μ) appears to be insensitive to sliding velocity. The values of μ for a particular composition of lead are almost constant or vary in a small range. The average value of coefficient of friction for the range of sliding velocity investigated for the Al–10Si–3.5Cu alloy is 0.376, whereas, the coefficient of friction has reduced to a minimum of 0.199 for the alloy with 30% Pb dispersion. The trend of reduction in μ with lead content for sliding velocity is similar to that observed for applied pressure, i.e. a large reduction in μ is observed for the alloy with 20% Pb dispersion for both the applied pressure as well as for the sliding velocity.

The temperature generated at the sliding surface becomes of paramount interest in understanding the wear
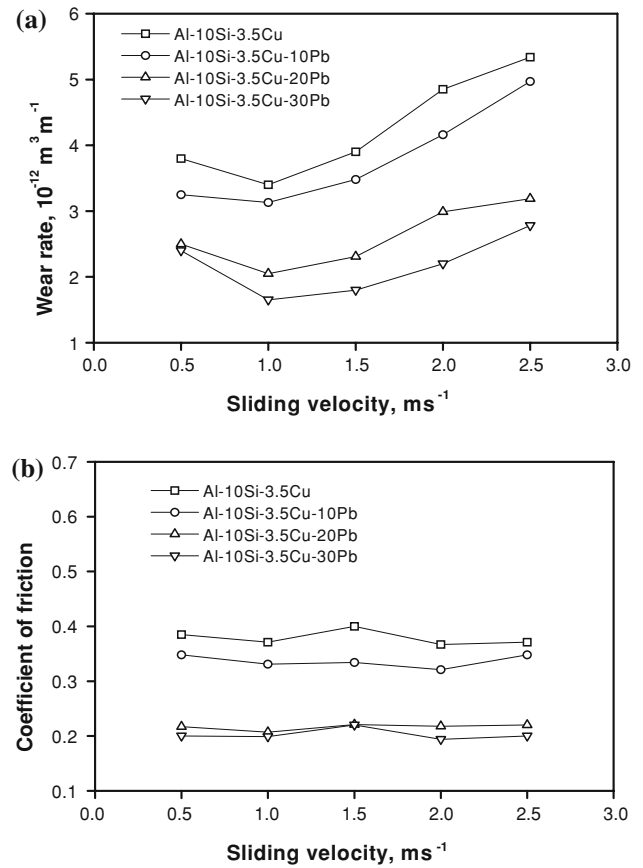
mechanism. We measured the temperature of the samples during wear and it is shown in Fig. 6. Figure 6a shows the variation in bulk temperature of the wear test specimen with applied load. These were evaluated at constant sliding velocity of 1.0 ms^{-1} for a sliding distance of 1,500 m for both the alloys with and without lead dispersions. The above figure depicts that the bulk temperature of the test pin rises with increase in applied pressure. The rise in temperature has almost linear relationship for the alloys with Pb dispersion with increase in pressure. However, a steep rise is observed for base alloy after an applied pressure of 0.6 MPa. A rise in temperature of 9 °C is recorded at an applied pressure of 0.2 MPa for the base alloy. On the other hand, a rise in temperature of 48 °C is recorded at an applied pressure of 1.8 MPa for this alloy. The lead dispersed alloys exhibit lower rise in temperature compared to the base alloy. The alloy with 30% Pb dispersion shows minimum rise of temperatures of 3 and 23.7 °C at 0.2 and 1.8 MPa pressures, respectively, in the present investigation. Figure 6b shows the bulk temperature of the specimen recorded for the Al–3.5Cu–10Si base alloy as well as for that of alloy with varying lead dispersions for a sliding
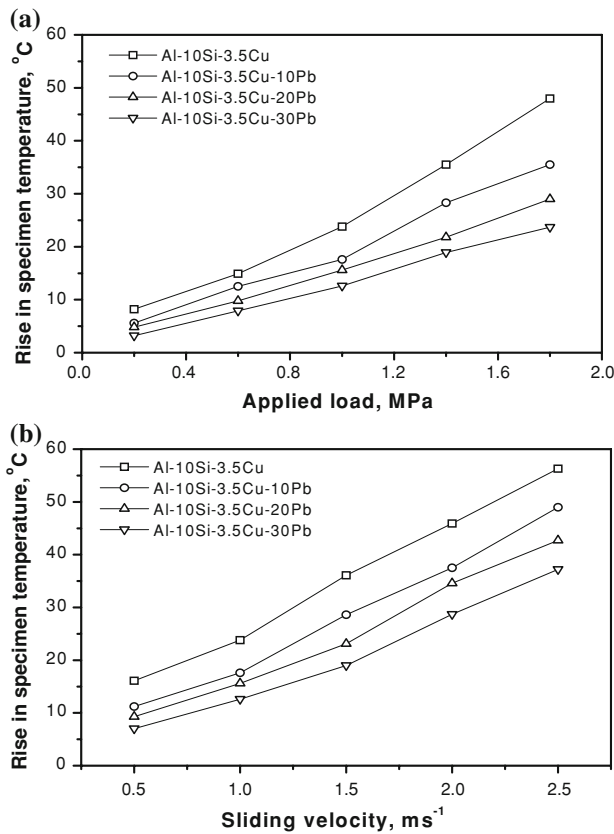
(a)

(b)

Fig. 6 Variation of rise in specimen temperature with (**a**) applied pressure, constant sliding velocity of 1.0 ms^{-1} and (**b**) with sliding velocity, constant applied pressure of 1.0 MPa

(a)

(b)

Fig. 7 Variation of (**a**) wear rate and (**b**) coefficient of friction with applied pressure for spray formed Al–Si alloys (constant sliding velocity of 1.44 ms^{-1})

distance of 1,500 m at various sliding velocities. The bulk temperature increases with increasing sliding speed. It should be noted that above 1.0 ms^{-1} the temperature rise with increasing sliding speed is steeper than that below it. This sliding speed of 1.0 ms^{-1} may be correlated to the critical speed at which a transition in the wear behaviour is noted as seen earlier. A rise in bulk temperature of 40 °C is observed for Al–3.5Cu–10Si base alloy for the range of sliding velocity between 0.5 and 2.5 ms^{-1}. On the other hand, there is a rise of 20 °C for the alloy with 30% Pb dispersion.

Al–Si alloys

The wear rate variation of spray formed Al–Si alloys with applied pressure is shown in Fig. 7a. It is depicted that the wear rate of the Al–6.5Si alloy increases almost linearly with increasing applied pressure. The wear rate varies between 1.5 and 7.5 × 10^{-12} m^3 m^{-1} for a range of applied pressures between 0.4 and 2.0 MPa. The wear rates of Al–18Si and Al–18Si–5Fe–1.5Cu alloys are consistently lower than that for the Al–6.5Si alloy. However, the wear rates of the former two alloys are comparable in the lower
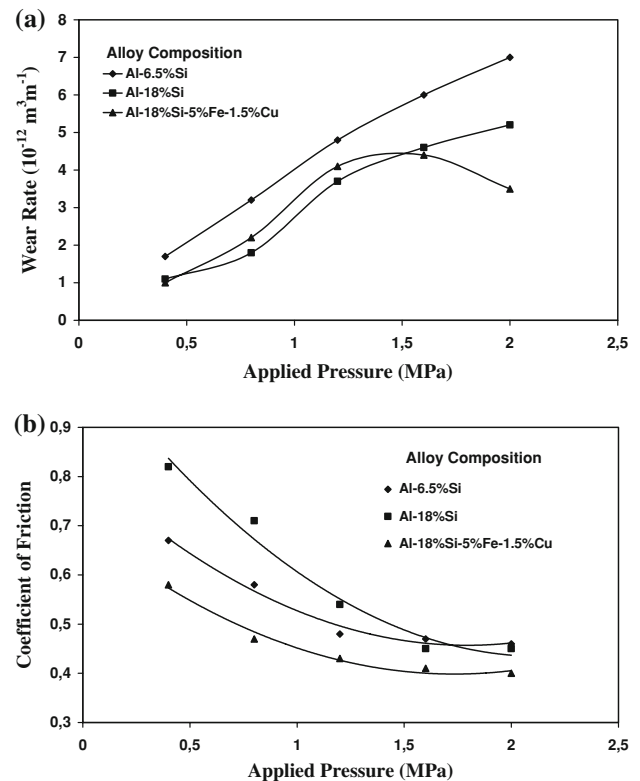
pressure range. Although the Al–18Si–5Fe–1.5Cu alloy shows a slightly higher wear rate at 0.8 and 1.2 MPa pressures compared with the Al–18Si alloy, the wear rate suddenly decreases at high pressures.

Figure 7b shows the variation in the coefficient of friction (μ) for alloys with applied pressure at a constant sliding speed of 1.44 ms^{-1}. This reveals a decreasing trend in the coefficient of friction with increasing applied pressure, for all alloys. However, the value of μ becomes relatively constant in the high pressure regime. It is evident from Fig. 7b that the difference in μ for all the alloys becomes smaller as the applied pressure is increased. The value of μ seems to decrease faster for the Al–18Si alloy compared with the Al–6.5Si and Al–18Si–5Fe–1.5Cu alloys. The average coefficient of friction is highest for Al–18Si alloy and lowest for the Al–18Si–5Fe–1.5Cu alloy.

2014-Al + SiC composites

The wear behaviour of spray formed composites is shown in Fig. 8. Figure 8a shows the wear rate for composites, having different reinforcement sizes and volume fractions, with applied pressure. It depicts clearly that the composites have lower wear rate compared to their un-reinforced base alloy. The wear rate of composites increases almost
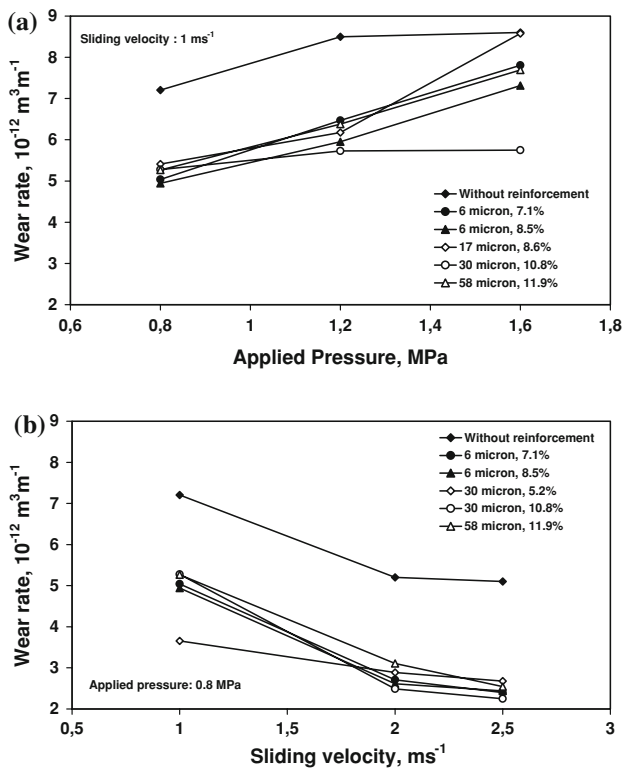
Fig. 8 Variation of wear rate of composites with (**a**) applied pressure and (**b**) sliding velocity

Fig. 9 The variation of sliding surface temperature with sliding distance (2 mm away from the sliding surface)

sliding distance. The figure depicts that a temperature of 55 and 80 °C is reached at 1.0 and 2.0 ms^{-1}, respectively, for composite with 8.6% of 17 μm size reinforcement. However, temperature increased further for the composite with 10.8% of 30 μm particles. However, these temperatures are underestimated as the temperature has been measured 2 mm away from the sliding surface, as mentioned in the "Experimental" section.

Discussion

Spray formed microstructure

The above discussed alloys pose difficulties during processing by conventional casting route. The spray forming route, which utilized the melt atomization to disintegrate the melt into small droplets with their subsequent deposition on a substrate, gave rise to refined and modified microstructural features of the alloys and composites [13, 15, 20, 21]. These microstructural features are generally not achievable by conventional casting processes. The major advantage has been derived in obtaining this microstructures is the rapid solidification effect on droplets and an unique mechanism of microstructural evolution during and after their deposition on the substrate [13]. The disintegration of liquid metal into micron size droplets limits the segregation possibility of different phases. The deposition of high velocity semi-solid/liquid droplets on the substrate gives rise to a highly turbulent liquid pool on the growing surface leading to fragmentation of dendrites and other solid phases. The debris created from the dendrite fragmentation leads to a large number of heterogenous nucleation sites which finally engender refined microstructure [20]. The relatively high cooling rate of the deposit does not allow further growth of second phase. Therefore, a refined and modified structure is obtained. The problems of segregation after adding Pb and SiC increases due to large density difference of Pb and

linearly with the applied pressure. However, there is no any specific trend observed with variation in reinforcement particle size and their volume fraction. The difference in wear rate of different composites, particularly at higher applied pressure, increased. This indicates a change in the wear mechanism at high pressure. The overall metal removal rate (i.e. wear rate) seems to be higher than that observed for Al–Si alloys and alloys added with Pb.

The effect of change in sliding velocity on the wear rate of composites is shown in Fig. 8b. It indicates that an increase in sliding velocity considerably affects the wear rate. The wear rate decreases sharply with increase in sliding velocity for composites with relatively higher volume fraction. However, even with increasing sliding velocity, the un-reinforced alloy showed higher wear rate compared to composites. The wear rate of composites become comparable to the un-reinforced alloys, discussed in the previous section, particularly at higher sliding speeds. This gave an indication that composites are not suitable for low sliding velocities. However, rate of decrease in wear rate with sliding velocity decreases as the velocity increased from 2.0 to 2.5 ms^{-1}.

Figure 9 shows the variation of sliding surface temperature for different composites and sliding velocities. It is observed that the temperature increases rapidly in the initial stage and then becomes steady approximately 500–600 m
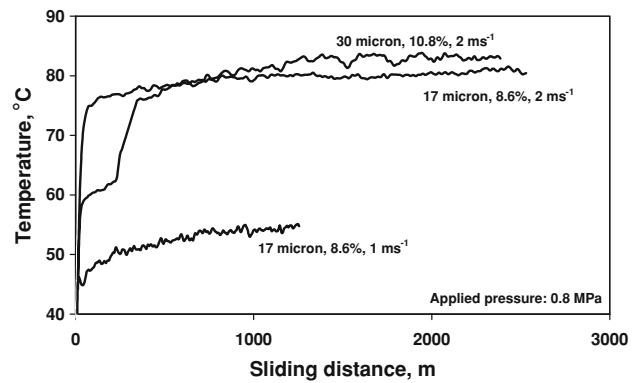
non-wettability of SiC by aluminium melt. However, this limitation is obviated in the spray forming process [4, 17]. The major advantage of spray forming is derived in incorporation of smaller SiC particles into matrix, which occurs due to collision of SiC particles with liquid droplets and their subsequent attachment/penetration in the droplet. This makes it possible to incorporate smaller particles with larger droplets on the deposition surface. A detailed analysis of microstructural evolution mechanism in composites can be seen in Ref. [17]. The presence of intragranular Pb particles in the spray formed Al–Si–Cu alloy has been observed and is attributed to high cooling rate of droplets in the spray. A high cooling rate leads to a large undercooling of droplets and therefore, a high solidification front velocity during solidification of primary Al phase. And also, during cooling of droplets, Pb droplets are phase separated into fine droplets in the parent liquid. As the solidification front advances rapidly, small Pb droplets are entrapped in the grains of primary phase. However, Pb would be in liquid state. If semi-solid/liquid droplets do not break during deposition, Pb particles remain in the matrix phase in solid deposit. This is against the equilibrium cooling condition where Pb droplets are pushed away from the solidification front and no intragranular Pb is observed.

Wear characteristics of alloys

The wear of materials between two relatively sliding contact surfaces is the result of the complex interplay between several mechanisms operating simultaneously. At the commencement of sliding, the surface of the sample undergoes severe deformation up to a few microns depth into the sample. This depth is known as the sub-surface layer. The phenomena occurring in the sub-surface layer basically determines the wear behaviour of materials [33, 34]. In general, the wear during dry sliding takes place by locking and local welding of surface asperities. However, in some cases, three-body abrasion may lead to ploughing action of material removal. The addition of Pb in Al–10Si–3.5Cu alloy with its uniform distribution due to spray processing improves the wear resistance [27]. The soft Pb is smeared over the sliding surface and in turn reduces the contact area between the specimen and the counterface and leads to easy shearing during sliding between two surfaces. Although the wear resistance of alloy containing 10%Pb decreased, it might not have given fully established smearing at the interface. However, the wear resistance increases sharply for 20%Pb. But there is not much effect for 30% Pb content. This may be attributed to the fact that only a slight layer of the smeared phase is enough to avoid surface contacts. However, an increase of 10%Pb may only increase the smeared layer thickness. There is similar the reason for reduced coefficient of friction (μ) of the alloying

containing 20%Pb. The high value of μ at applied pressure of 0.2 MPa may be attributed to only locking of surface asperities. An increased pressure leads to deformation, welding and re-welding of asperities, establishing a planar contact. A low value of Pb content, asperity/protrusion locks cannot be avoided. As we can see from Fig. 6, the temperature rise of the specimen decreases with the increasing Pb content. This is also an indicative of the less energy input in the specimen during sliding in terms of material deformation and breaking of welded asperities. This is possible only if an easy shear action takes place between the contacting surfaces. Figure 10 shows the topography of worn specimen surfaces. At low load of 0.6 MPa, it seems that the Pb particles are fully smeared on the worn surface along with oxide particles (Fig. 10a). However, at high load of 1.8 MPa, large grooves are seen indicating metallic wear (Fig. 10b). At higher load the thin Pb layer breaks giving rise to full metal–metal contact between sliding faces. Similarly, at low speed of 0.5 ms^{-1}, worn surfaces were seen to have oxide particles and Pb smeared over the surface which makes the shearing easier. Whereas, at higher speed of 2.5 ms^{-1}, the worn surface showed compacted patches of separated material resulting from transfer and back transfer of the material (Fig. 10d).

The wear behaviour of Al–Si alloys is basically governed by the size and content of Si particles. A higher Si content in Al–18Si alloy leads to a better wear resistance compared to Al–6.5Si alloy [35]. The extensive refinement of primary Si phase may also be attributed to this behaviour. It has been observed by several investigators that smaller the size of Si particles better would be the wear resistance [34, 36]. A large particle size exposes a smaller surface area, because of the small specific surface area in contact with the matrix, to the matrix material that renders a poor overall interface bonding. The interfacial regions between the Si particles and the matrix, therefore, become prone to micro-cracking, i.e. the larger the size of Si particle the larger will be the probability of micro-cracking at the interface. As a result, large sized Si particles peel out from the matrix and leave bare matrix in contact with the counter-surface during the wear process. The spray formed alloys that have a fine and uniform distribution of primary Si phase, therefore, invariably show increased wear resistance. It was observed that porosity present in the Al–18Si–5Fe–1.5Cu alloy was higher compared to Al–18Si alloy. However, the wear rate of the alloys is similar in the low pressure regime, whereas there is a sudden decrease in the wear rate of the Al–18Si–5Fe–1.5Cu alloy at the higher pressure of 1.6 MPa. This difference in wear rate at higher applied pressure could be attributed to the formation of some thermally stable intermetallic compounds in the Al–18Si–5Fe–1.5Cu alloy such as Al$_3$Fe, β-Al$_5$SiFe and δ-Al$_4$Si$_2$Fe [32]. At higher pressure, when the temperature

Fig. 10 Morphology of worn out surfaces of Al–3.5Cu–10Si–20Pb spray deposited alloy at a sliding velocity of 1.0 ms^{-1} for (**a**) 0.6 MPa, (**b**) 1.8 MPa, (**c**) 0.5 ms^{-1} and (**d**) 2.5 ms^{-1}
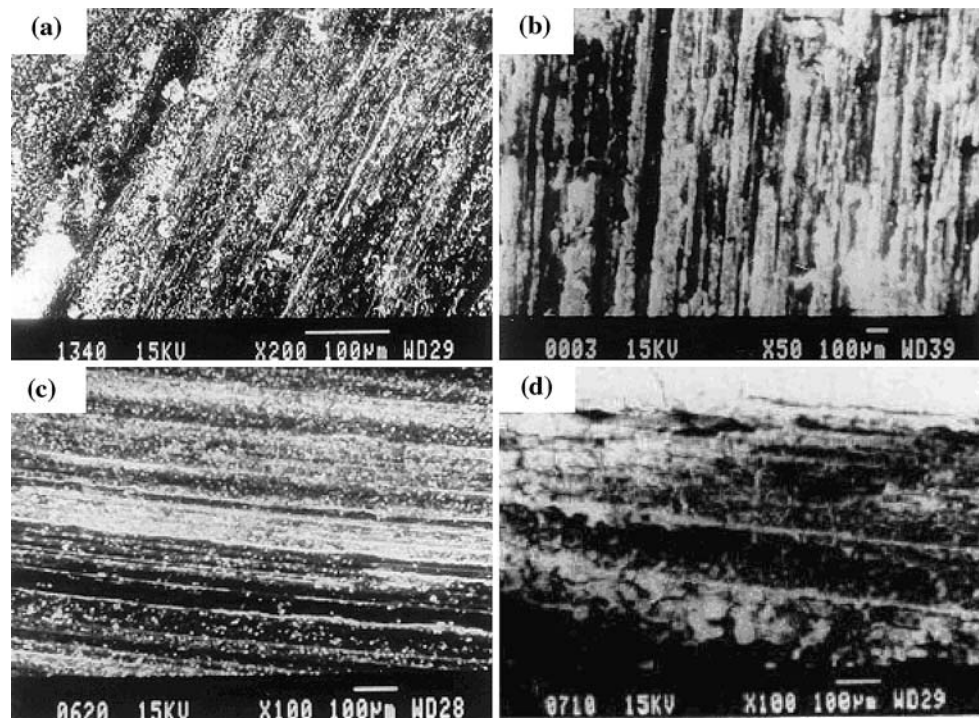
of the contact surface rises, the material softens and the flow stress of the materials decreases leading to increased wear rate. The uniform distribution of thermally stable compounds in the Al–18Si–5Fe–1.5Cu alloy is supposed to hamper severe plastic flow and maintains the wear resistance of the alloy. It was observed in this study that coefficient of friction μ is sensitive to the applied pressure and composition of the alloys. At low applied pressures, the pin and counter surface do not make full metallic contact and μ is, therefore, governed by the combined effect of oxidation and adhesion of the small protrusions on the contacting surfaces. With the increase in the applied pressure, the surface contact area also increases and the values of μ become closer to each other for different alloys. A narrow range of variation of μ at higher pressures, therefore, can be attributed to the fact that all the alloys have aluminium as a major fraction. A high pressure on the surface makes it possible for the matrix aluminium from the specimen and counter-surface to be in contact. This, therefore, determines the effective coefficient of friction.

Wear characteristics of composites

The wear resistance of composites generally depends upon the size and volume fraction and type of reinforcement particles. However, due to the poor interface characteristics of the Al matrix and SiC particles, and inherent porosity in as-cast and spray formed materials, the fundamental study of the operating wear mechanism becomes a difficult proposition. However, some studies have been carried out to

evaluate the wear response of spray formed composite materials [28, 37]. It has been observed, in the present study, that the composites do show improved wear resistance compared to their un-reinforced counterpart at low applied pressure. But it was difficult to find the exact parameter leading to the observed behaviour. In general, at low applied pressure the reinforcement particles support the load. And, as the particles are hard, the wear resistance of the composites is superior to their monolithic counterparts [38]. A similar behaviour was observed in the present study also. However, as the applied pressure increases, the particles in the composites sample starts peeling out and act as third body abrasive. There are possibilities that the particles may also refine due to high compressive stresses and may get embedded in the subsurface layer. However, both the phenomena may go together. Therefore, the wear rate of the composite increases. However, with further increase in the applied load, the interface temperature increases leading to softening of the matrix phase. Alpas and Zhang [38] have demonstrated that a temperature of 127 °C is the critical temperature for 6061Al for commencement of severe wear regime. However, in the present study, it was observed that at 1 ms^{-1} sliding velocity and 1.6 MPa applied pressure, the temperature reaches to 50–60 °C, which is not as high a temperature to lead to severe wear. The soft matrix with low shear resistance and also the peeling out of the particles from the matrix aids to wear. Whereas, mechanical mixing of particles in the subsurface layer may resist wear. In addition, porosity present in the samples acts as crack initiation points and leads to fracture and delamination [37]. As the porosity

increases with increasing volume fraction and decreasing size of reinforcement particles in the spray formed composites, it is expected that composites with large size particle may give rise to better wear resistance. However, very large size particle reduces the number of particles for a given volume fraction and therefore, the load bearing area becomes smaller, which in turn increases the pressure on particles. This may lead to poor wear resistance. However, it may be considered that the there is a threshold porosity level in composites which is engendered by the process parameters used in spray forming process. The increased sliding velocity leads to reduction in the wear rate in the low pressure regime of 0.8 MPa. At higher sliding velocity, the bulk specimen temperature reaches to 80–90 °C and it is even higher for large size particles. This indicates that the matrix becomes softer and embedding of particles in the matrix becomes easy, which in turn lead to better load bearing capability. And also, the larger third body abrading

particle may go out of wear track due to higher centrifugal forces. The softening of the matrix may also help in filling up the pores and reducing the wear caused due to premature fracture and delamination. However, still higher velocity of 2.5 ms^{-1} does not help in increasing the wear resistance considerably. This may be attributed to further increase in specimen temperature and matrix softening. The effect of embedded particles may reduce, when the matrix becomes softer.

Figure 11 shows the topography of worn surfaces of different specimens worn at 1.6 MPa pressure and 1.0 ms^{-1} sliding velocity. Figure 11a shows the large grooves in the base alloy indicating a metallic wear. Whereas, in some regions delamination could also be seen (Fig. 11b). In the composite with 6 μm particles, small size grooves are seen with oxide patches and discontinuous ridges (Fig. 11c). This indicates typical abrasive wear of these samples. Evidence of delamination and fracture is

Fig. 11 Topography of worn surfaces of specimens at 1.6 MPa applied pressure and 1.0 ms^{-1} sliding velocity (**a**, **b**) Base alloy 2014 Al (**c**, **d**) composite; 6 mm; 8.5%; (**e**, **f**) composite; 58 mm; 11.9%
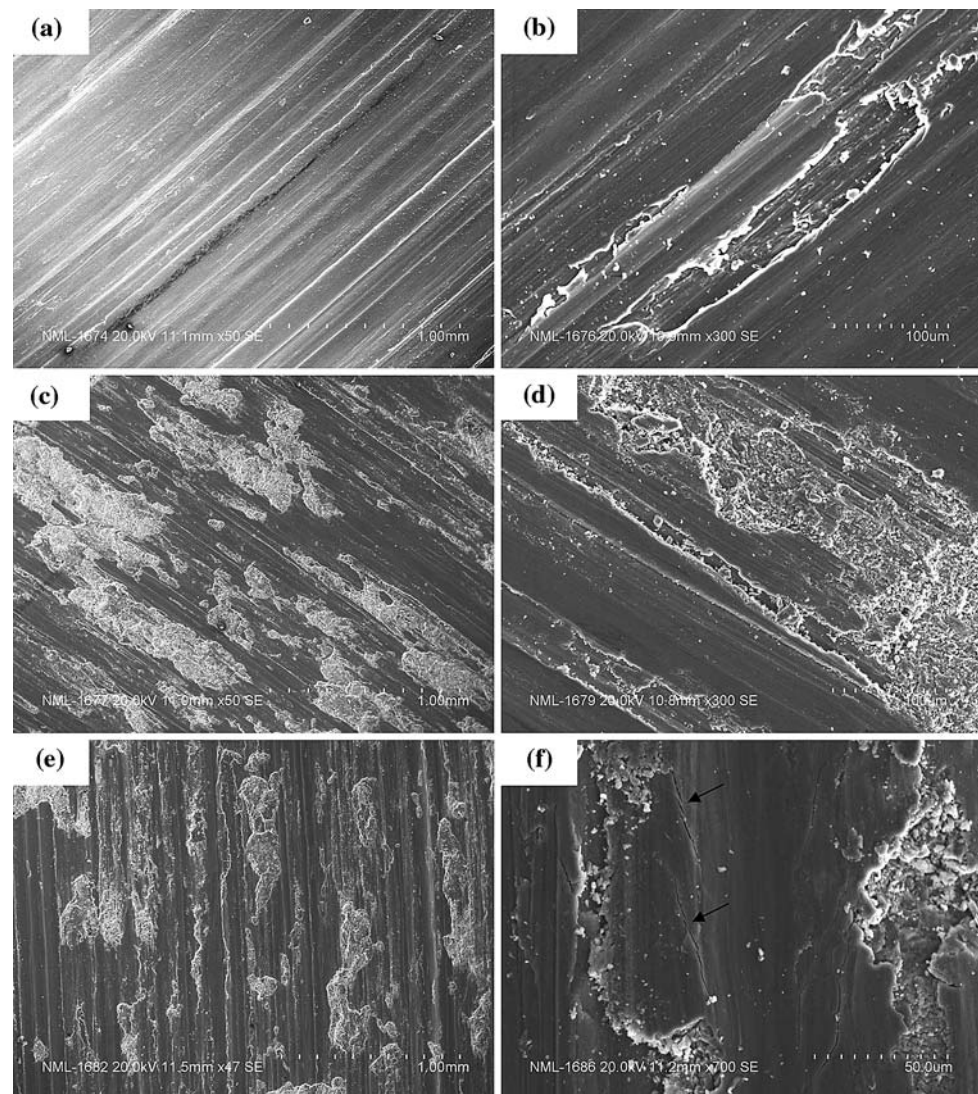
also observed in these samples (Fig. 11d). However, there was no trace found for cracking of the matrix. In the composite with 58 μm particles, the width of the grooves seemed to increase, which is can be the result of large size particle reinforcement (Fig. 11e). In this composite, the cracking of layers could be seen. It may be possible that the third body abrasion with peeled out large size particles gives rise to severe deformation of the matrix phase and causes it to crack. This crack formation may eventually lead to faster material removal.

Conclusions

The following conclusions can be drawn from the work of the present investigation:

(1) Spray forming process facilitates effective microstructural modification during processing of liquid immiscible Al–Pb based alloys, Al–Si alloys as well as Al based SiC reinforced metal matrix composites. This was achieved due to modification in Pb and SiC incorporation techniques.

(2) The wear resistance of Pb reinforced alloys increases with increase in the Pb content. However, the addition of more than 20%Pb does not improve the wear resistance considerably. The wear rate becomes half compared to that of the monolithic Al–10Si–3.5Cu alloy.

(3) The addition of SiC particles as reinforcement phase improves the wear resistance of 2014Al alloy. However, the reinforcement does not give rise to any advantage over monolithic alloy at higher applied pressure. The wear rate decreases with increase in the sliding velocity.

(4) The alloying addition of Fe and Cu in Al–18Si alloy improves the wear resistance at higher applied pressure due to the presence of thermally stable intermetallic compounds.

References

1. Roberts EW (1990) Tribol Int 23:95. doi:10.1016/0301-679X(90)90042-N
2. Mohan S, Agarwala V, Ray S (1992) Wear 157:9. doi:10.1016/0043-1648(92)90184-A
3. Alkemper J, Ratke L (1994) Z Metallk 85:365
4. Rudrakshi GB, Srivastava VC, Ojha SN (2007) Mater Sci Eng A 457:100. doi:10.1016/j.msea.2006.12.024
5. Lloyd DJ (1994) Int Mater Rev 39:1
6. Ratke L, Diefenbach S (1995) Mater Sci Eng Rep 15:1. doi:10.1016/0927-796X(95)00180-8
7. Al-Rubaie KS, Goldenstein H, De Mello JDB (1999) Wear 225–229:163. doi:10.1016/S0043-1648(99)00009-5
8. Bindumadhavan PN, Chia TK, Chandrasekaran M, Wah MK, Lam NK, Prabhakar O (2001) Mater Sci Eng A 315:217
9. Muratoglu M, Aksoy M (2006) J Mater Proc Tech 174:272. doi:10.1016/j.jmatprotec.2006.01.010
10. Tenekedjiev N, Gruzleski JE (1990) Cast Metab 3:96
11. Jorstad JL (1971) AFS Trans 79:85
12. Midling OT, Grong O (1995) Key Eng Mater 104–107:329
13. Srivastava VC, Mandal RK, Ojha SN (2004) Mater Sci Eng A 383:14. doi:10.1016/j.msea.2004.02.031
14. Wu Y, Lavernia EJ (1992) Metab Mater Trans A 23:2923. doi:10.1007/BF02651770
15. Wu Y, Cassada WA, Lavernia EJ (1995) Metab Mater Trans A 26:1235. doi:10.1007/BF02670618
16. Chiang CH, Tsao CYA (2005) Mater Sci Eng A 396:263. doi:10.1016/j.msea.2005.01.017
17. Srivastava VC, Schneider A, Uhlenwinkel V, Bauckhage K (2005) Mater Sci Eng A 412:19
18. Tham LM, Gupta M, Cheng L (1999) J Mater Process Technol 89–90:128. doi:10.1016/S0924-0136(99)00002-3
19. Zambon A, Badan B, Maddalena A (2004) Mater Sci Eng A 375–377:645. doi:10.1016/j.msea.2003.10.229
20. Lavernia EJ, Wu Y (1996) Spray atomization and deposition. Wiley, West Sussex, England
21. Grant PS (1995) Prog Mater Sci 39:497
22. Srivastava VC, Schneider A, Uhlenwinkel V, Ojha SN, Bauckhage K (2005) Trans Ind Inst Met 58:91
23. Ojha KV, Tomar A, Singh D, Kaushal GC (2008) Mater Sci Eng A 487:591
24. Lim SC, Gupta M, Leng YF, Lavernia EJ (1997) J Mater Proc Tech 63:865
25. Elmadagli M, Perry T, Alpas AT (2007) Wear 262:79
26. Srivastava VC, Ojha SN (2004) Mater Sci Tech 20:1632
27. Gouthama, Rudrakshi GB, Ojha SN (2007) J Mater Proc Tech 189:224
28. Chen Z, Teng J, Chen G, Fu D, Yan H (2007) Wear 262:362
29. Lim SC, Gupta M, Ren L, Kwok JKM (1999) J Mater Proc Tech 89–90:591
30. Schneider A, Srivastava VC, Uhlenwinkel V, Bauckhage K (2004) Z Metallk 95:763
31. Srivastava VC, Mandal RK, Ojha SN, Venkateswarlu K (2007) Mater Sci Eng A 471:38
32. Srivastava VC, Ghoshal P, Ojha SN (2002) Mater Lett 56:797
33. Hirst W, Lancaster JK (1956) J Appl Phys 27:1057
34. Davis FA, Eyre TS (1994) Tribol Int 27:171
35. Antoniou A, Boraland DW (1987) Mater Sci Eng A 93:57
36. Amateau MF, Lee DS, Conway JC (1996) In: Wood JV (ed) Proc 3rd Int Conf 'Spray forming' (ICSF-3). Cardiff, UK, p 321
37. Gui M, Kang SB, Lee JM (2000) Mater Sci Eng A 293:146
38. Alpas AT, Zhang J (1999) Metall Mater Trans A 25:969